EUROPEAN ORGANIZATION FOR NUCLEAR RESEARCH

CERN/EP 85-118
27 July 1985

INCLUSIVE PROPERTIES OF D-MESONS PRODUCED IN 360 GeV π^-p INTERACTIONS

NA27 LEBC/EHS Collaboration

Aachen[1]-Bombay[2]-Brussels[3]-CERN[4]-Collège de France[5]-Genova[6]-Japan Universities[7]-(Chuo University, Tokyo Metropolitan University, Tokyo University of Agriculture and Technology)-Liverpool[8]-Madrid[9]-Mons[10]-Oxford[11]-Padova[12]-Paris[13]-Roma[14]-Rutherford[15]-Rutgers[16]-Serpukhov[17]-Stockholm[18]-Strasbourg[19]-Tennessee[20]-Torino[21]-Trieste[22]-Vienna[23] Collaboration

M. Aguilar-Benitez[9], W.W. Allison[11], J.F. Baland[10], S. Banerjee[2], W. Bartl[23], P. Beillère[5], M. Bengalli[1], G. Borreani[21], R. Bizzarri[14], H. Briand[13], R. Brun[4], W.M. Bugg[20], C. Caso[6], B. Castano[9], E. Castelli[22], P. Checchia[12], P. Chliapnikov[17], S. Colwill[11], R. Contri[6], D. Crennell[15], M. Cresti[12], A. De Angelis[12], L. De Billy[13], Ch. Defoix[5], E. Di Capua[14], R. Di Marco[16], J. Dolbeau[5], J. Dumarchez[13], S. Falciano[14], C. Fernandez[4], C.M. Fisher[15], Yu. Fisjak[17], F. Fontanelli[6], J.R. Fry[8], U. Gasparini[12], S. Gentile[14], A.T. Goshaw[4], F. Grard[10], A. Gurtu[4], T. Handler[20], R. Hamatsu[7], E.L. Hart[20], L. Haupt[18], S. Hellman[18], J. Hernandez[4], A. Hervé[4], S.O. Holmgren[18], M.A. Houlden[8], J. Hrubec[23], P. Hughes[15], M. Iori[14], E. Jegham[19], E. Johansson[18], E. Kistenev[17], S. Kitamura[7], D. Kuhn[23], V. Knjasev[17], A.I. Kurnosenko[17], P. Ladron de Guevara[9], M. Laloum[5], H. Leutz[4], P. Lutz[5], L. Lyons[11], M. MacDermott[15], P.K. Malhotra[2], F. Marchetto[21], G. Marel[14], J.Cl. Marin[4], F. Marzano[14], P. Mason[8], M. Mazzucato[12], A. Michalon[19], M.E. Michalon-Mentzer[19], T. Moa[18], L. Montanet[4], J. Morton[8], G. Neuhofer[23], H. Nguyen[13], S. Nilsson[18], H. Nowak[4], N. Oshima[7], G. Otter[1], G.D. Patel[8], M. Pernicka[23], P. Pilette[10], C. Pinori[12], G. Piredda[14], R. Plano[16], A. Poppleton[4], P. Poropat[22], R. Raghavan[2], G. Ransone[1], S. Reucroft[4], J. Richardson[4], S. Rinaudo[21], K. Roberts[8], H. Rohringer[23], H. Schlütter[1], J. Schmiedmayer[23], R. Schulte[1], W. Struczinski[1], M. Schouten[4], B. Sellden[18], M. Sessa[22], K. Shankar[2], P. Stamer[16], K.M. Stopchenko[17], Struczinski[1], S. Squarcia[6], A. Subramanian[2], K. Takahashi[7], M.Cl. Touboul[4], U. Trevisan[6], C. Troncon[22], T. Tsurugai[7], P. Vilain[3], B. Vonck[3], B.M. Whyman[8], J. Wickens[3], C. Willmott[9], P. Wright[11] and G. Zumerle[12]

Submitted to Physics Letters B

2718P/CMF/ed

ABSTRACT

The inclusive cross sections for forward D meson production at $\sqrt{s}$ = 26 GeV in $\pi^- p$ interactions have been measured to be:

$$\sigma(\pi^- p \to D^0/\bar{D}^0 + X)_{x_F>0} = (10.1 \pm 2.2)\mu b$$

$$\sigma(\pi^- p \to D^{\pm} + X)_{x_F>0} = (5.7 \pm 1.6)\mu b$$

The distribution in x_F for all D and for $x_F > 0$ has the form

$$\frac{d\sigma}{dx_F} = 107^{+39}_{-37}(1- x_F)^{7.5^{+2.5}_{-1.7}} + 5.4^{+6.0}_{-3.8}(1 - x_F)^{0.7^{+1.0}_{-0.7}} \mu b.$$

with evidence for leading D production. The p_T^2 distribution is exponential with slope parameter $[-1.18^{+0.18}_{-0.16}](GeV/c)^{-2}$. The data are compared with predictions from first order quark/gluon fusion calculations.

We report the results of a study of the inclusive properties of charm D-mesons produced in 360 GeV π^-p interactions. The experiment was performed using the high resolution hydrogen bubble chamber, LEBC, in association with the European Hybrid Spectrometer (EHS). A detailed description of the experimental set up and the data analysis procedure is given in ref. [1].

The data were obtained by direct observation of the decays of charm particles produced in π^- interactions in hydrogen using a minimum bias interaction trigger [1]. Losses occur only in low multiplicity peripheral events and are negligible for the charm sample discussed below. The spectrometer acceptance rises sharply at $x_F = 0$ to ~ 100% for the charged decay products of D-mesons and this results in an essentially unbiased sample of decays for $x_F > 0$, where $x_F = p^*_{//}/p^*_{//max}$ is the Feynman variable.

The experiment differs from that reported in ref. [2] in three important respects:

(a) The bubble chamber has been redesigned to give improved resolution ($\leq$ 20 μm) and picture quality. This increases the sensitivity to short decays and substantially reduces topological ambiguities.

(b) The spectrometer has been upgraded to include charged particle identification via the large drift chamber ISIS [3] which allows the resolution of kinematical ambiguities between charm interpretations.

(c) The overall sensitivity is increased to (15.8 ± 0.8) events/μb.

We refer to ref. [1] for all details of film analysis.

The data sample consists of 114 events containing 183 candidate charm decays: 69 pairs and 45 singles. The observed decay topologies can be classified as 28C1, 78V2, 51C3, 22V4 and 4C5 where Cn defines an n prong charged decay and Vn an n prong neutral decay. C1 decays have a poor scanning efficiency and often correspond to underconstrained decay fits with undefined production properties and are therefore not used in the

analysis. To eliminate strange particle decays and gamma conversions V2 candidates are accepted only if at least one of the tracks has $p_T > 250$ MeV/c and the opening angle is seen to be non zero in the bubble chamber. The residual background in the resulting charm sample is then estimated [1] to be less than 1 decay.

From this sample we derive the inclusive production cross sections for charm D mesons having $x_F > 0$ using the known topological branching ratios [4]. To ensure high scan efficiency (> 98% from two independent scans) at least one decay track is required to have impact parameter > 50 μm for neutral decays, or > 80 μm for charged decays. (The larger value chosen for charged decays is essentially a lifetime cut to remove possible Λ_c contamination of the $D^{\pm}$ sample). To remove the topological ambiguity between the C3 topology and a V2 superimposed on a track from the primary vertex, the minimum impact parameter is required to be greater than 7 μm for a V2 and greater than 10 μm for a C3 decay. All the V4 or C5 decays give kinematic solutions with well defined x_F, however, V2 and C3 decays often have ambiguous multineutral solutions such that x_F is not well determined. In order to compute the cross section for $x_F > 0$ we therefore impose the condition that the visible longitudinal momentum of the charged decay products is greater than 16 GeV/c for V2 and greater than 20 GeV/c for C3 decays. A Monte-Carlo study shows that with these cuts 6% of decays having $x_F < 0$ are included and 7% of decays having $x_F > 0$ are lost, assuming symmetric production in the central region.

A visibility weight is applied to the resulting sample to obtain an absolute cross section and this weight depends on the value of the particle lifetime. We have used the current world average lifetimes [5] $\tau(D^0) = (4.3 \pm 0.4) \times 10^{-13}$ s and $\tau(D^{\pm}) = (9.1 \pm 1.1) \times 10^{-13}$ s, and the topological branching ratios [4] $D^0 \rightarrow V2 + V4 = (84 \pm 8)\%$ and $D^{\pm} \rightarrow C3 + C5 = (46 \pm 10)\%$.

We then obtain, for $\sqrt{s} = 26$ GeV,

$$\sigma(\pi^- p \rightarrow D^0/\bar{D}^0 + x)_{x_F>0} = (10.1 \pm 2.2)\mu b$$

based on 48 events surviving all cuts and

$$\sigma(\pi^- p \to D^{\pm} + x)_{x_F>0} = (5.7 \pm 1.5)\mu b$$

based on 14 events surviving all cuts.

Further details of this analysis, which is in good agreement with NA16 [2], are given in [1].

Before discussing the differential production distributions we note that clear evidence for D^* production is observed. The D^* analysis is reported elsewhere [6] where it is shown that more than 50% of the D-mesons are produced via D^*. This result readily accounts for the difference between the observed $D^o/\bar{D}^o$ and $D^{\pm}$ cross sections reported above.

To study the differential distributions, only those decays having well determined x_F and p_T are considered. This is achieved by the use of kinematic fits to decay channels with particle identification probabilities included to resolve ambiguities where possible. Residual ambiguities are treated by applying simple overall constraints to the event to arrive, where possible, at a unique solution. The constraints used are:

(a) The total event energy, including missing neutrals required for decay fits, should not exceed 360 GeV.

(b) If the charm content of one decay has been established, for example via a well constrained fit or by identifying a charged K or lepton, then the other decay of the pair must balance charm.

(c) Cabibbo favoured solutions are preferred over unfavoured solutions of the same constraint class, and D solutions are preferred over equivalent F or Λ_c solutions not resolved by particle identification.

(d) Ambiguous missing neutral solutions are treated as follows. For each decay the maximum missing mass is calculated using

$$M_o^2 = m_i^2 + m_c^2 - 2m_i\,(m_c^2 + p_T^2)^{1/2}$$

where m_i is the mass of the decaying particle (i.e. D meson) and m_c, p_T are the effective mass and resultant transverse momentum of all charged particles in the decay. If $M_o + \Delta M_o < 400$ (700) MeV/c^2 the decay is considered as a candidate for a single missing π^o (K^o) solution. If $M_o + \Delta M_o > 400$ (700) MeV/c^2 the event is classified as a probable multineutral decay ($\pi^o\pi^o$ ..., $K^o\pi^o$ ...).

In general, 0C fits give two ambiguous single missing π^o (K^o) solutions. If the above missing mass cuts are satisfied, the probability that the decay gammas from the two solutions lie within the acceptance of the gamma detectors is calculated. In cases corresponding to very different ($\Delta x_F > 0.1$) values of the D momentum the detection probabilities for the two π^o solutions are also very different and the presence or absence of the appropriate gammas can be used to make a choice. Missing K^o solutions can be treated in the same way although in this case one of the solutions is often unphysical. A K^o solution is preferred if there is convincing evidence for the K^o decay in the spectrometer or a neutral hadron in the calorimeter at the required position.

Details of the particle identification procedure and the Monte-Carlo studies employed to arrive at the above criteria are given in [1]. It should be noted, however, that the procedure does not define unambiguous unique fits which could be used for decay studies but allows us to arrive at the most probable values for the production variables, and hence their inclusive distributions, presented in this paper. Statistical fluctuations are large compared with any residual systematic uncertainties arising from the above procedures [1].

Following these procedures we arrive at a sub-sample of 57 reconstructed decays with $x_F > 0$ and well determined production variables which are used in the following x_F and p_T studies. An additional 19 D decays have $x_F < 0$ and three C3 decays are identified as Λ_c's and are reported in [1]. Twenty one decays have multineutral solutions such that x_F and p_T are effectively undetermined and

therefore cannot be used, however, since their omission is on the basis of decay mode, this does not introduce a bias on the production variables. To construct the production distributions from the 57 decays used, each decay is assigned a weight derived from the spectrometer acceptance and the visibility in the chamber. Both weights are largely insensitive to the production variables x_F, p_T and are detailed in [1]. The essential features of the distributions are apparent in the unweighted data.

In fig. 1 we show the differential distribution in x_F for all D mesons having $x_F > 0$. The distribution can be fitted to the form $d\sigma/dx_F \propto (1-x_F)^n$ or to the invariant form $E\, d\sigma/dx_F \propto (1-x_F)^a$. For the total sample we find $n = 3.8 \pm 0.63$ and $a = 1.6^{+1.4}_{-1.0}$.

If we separate the sample into "leading" states corresponding to D-mesons containing a quark which could be a valence quark of the incoming pion (including the effects of D^* production) and "non-leading" states, which have no quark in common with the incident pion, we find very different behaviour. These distributions are shown in figs 2(b) and 2(a). Performing the non-invariant fit to $(1 - x_F)^n$ we find $n = 1.8^{+0.6}_{-0.5}$ for the "leading" sample and $n = 7.9^{+1.6}_{-1.4}$ for the "non-leading" sample. Note that the "leading" sample has four events with $x_F > 0.6$ two of which have $x_F > 0.8$ whilst the highest x_F in the "non-leading" sample is 0.40.

We are therefore led to try a two component fit to the full distribution for $x_F > 0$, of the form

$$\sigma = \sigma_o[\alpha \int (n_1 + 1)(1 - x_F)^{n_1} dx + (1 - \alpha) \int (n_2 + 1)(1 - x_F)^{n_2} dx]$$

where σ_o is the total cross section for x_F positive and α is the fraction of this cross section in the central component ($n_1 > n_2$). The cross section σ can be integrated over any range of x_F in the forward direction. We find $\alpha = 0.80^{+.11}_{-.18}$, $n_1 = 7.5^{+2.5}_{-1.7}$ and $n_2 = 0.7^{+1.0}_{-0.7}$. Normalising to the observed single particle inclusive cross section of 15.8 μb, the differential cross section has the form for $x_F > 0$:

$$\frac{d\sigma}{dx_F} = 107^{+39}_{-37}(1- x_F)^{7.5^{+2.5}_{-1.7}} + 5.4^{+6.0}_{-3.8}(1 - x_F)^{0.7^{+1.0}_{-0.7}} \mu b.$$

The so-called "leading" sample (D^-, D^o, D^{-*}, D^{o*}) should be populated by both centrally produced and leading states. A two component fit to this sample alone with the exponent n_1 fixed from the one component fit to the central distribution ($n_1 = 7.9$) yields $n_2 = 1.0^{+0.9}_{-0.7}$ and $\alpha = 0.37^{+0.26}_{-0.35}$. Although statistics are poor the leading effect in x_F is therefore clearly correlated with the leading quark states.

The transverse momentum distribution is particularly sensitive to possible scanning losses and reconstruction difficulties in the forward direction for complex events. To avoid any possible systematic bias against low p_T decays we therefore apply the maximum impact parameter cuts as described for the cross section determination. The surviving sample of 48 decays are used to study the p_T^2 distribution. The distribution is shown in fig. 3 and can be fitted to the form

$$\frac{d\sigma}{dp_T^2} \propto \exp\{-1.18^{+0.18}_{-0.16}\ p_T^2\}$$

with mean $\langle p_T^2 \rangle = 0.84\ (GeV/c)^2$.

The data can be compared with the predictions of the fusion model which might be expected to account for the production of $c\bar{c}$ pairs. Many calculations exist for $c\bar{c}$ production via gluon-gluon and quark antiquark fusion [7]; differences arise from the parton distributions used, the assumed values for the charm quark mass m_c and the strong interaction scale parameter Λ, and the form of the charm quark fragmentation function.

The data are compared here with the predictions from three such QCD fusion calculations. The proton and π^- parton distribution functions are taken from [8] and [9] and an intrinsic transverse momentum is given to the partons according to a Gaussian distribution of the form

$$\frac{dN}{dk_T^2} = \exp(-k_T^2/\langle k_T^2\rangle)/\langle k_T^2\rangle$$

where the average value of k_T^2, $\langle k_T^2\rangle$ is fixed at $0.64(\text{GeV/c})^2$ consistent with results from J/ψ and direct lepton hadroproduction [10]. The calculations differ in their treatment of the charm quark fragmentation. The fragmentation functions used are:

- Model 1: Hard fragmentation $f(z) = \delta(z_{max} - z)$.

- Model 2: Peterson fragmentation [11]

$$f(z) = \{z[1 - \frac{1}{z} - 0.15/(1 - z)^2]\}^{-1}$$

  where z is the ratio of the D or $\bar{D}$ momentum to the original c or $\bar{c}$ momentum in the parton parton subsystem.

- Model 3: The Lund fragmentation which takes account of the colour fields and the couplings to the valence quarks [12].

The $c\bar{c}$ cross section is derived from the hard parton collisions and is a function of the charm quark mass m_c and the parameter Λ, as discussed previously in refs [13] and [14]. The cross section also depends on the threshold value $\hat{s}_{TH}$ used in the integration of the $gg \to c\bar{c}$ and $q\bar{q} \to c\bar{c}$ subprocesses. If m_c and Λ are fixed at 1.25 GeV/c^2 and 0.2 GeV respectively the fusion model predictions for the inclusive charm cross section with $x_f > 0$ vary from 6 to 15 μb as $\hat{s}_{TH}$ varies from $4m_D^2$ to $4m_c^2$. Our measured cross section (15.8 ± 2.7 μb) for $D/\bar{D}$ production is therefore somewhat high compared with the first order QCD prediction, reminiscent of Drell-Yan calculations.

The shapes of the differential distributions in x_F and p_T are not strongly dependent on the above parameters. To compare the model predictions with the data all models are therefore normalised to 15.8 μb, the observed cross section for $x_F > 0$. In fact the hard fragmentation implies $m_c = m_D$ and will clearly give an unacceptably low cross section; it is included to illustrate the bare QCD predictions for the differential distribution shapes.

All three calculations reproduce reasonably well the central region of the x_F distribution; however, only the hard fragmentation and the Lund model succeed to fit the whole x_F distribution and the observed distribution in p_T^2. In figs 1 and 3 we give three curves: a solid curve representing the experimental fit to the data, a dashed curve representing the fusion model with hard fragmentation and a dotted curve representing the fusion model with the Lund fragmentation. In fig. 2 we show only the experimental fit and the Lund calculation (which predicts the leading and non-leading distributions separately). A two component fit to the x_F distribution for all D mesons predicted by the Lund Monte-Carlo yields $\alpha = 0.83$, $n_1 = 5.7$ and $n_2 = 1.4$. A single component fit yields $n = 5.7$ for the non-leading states and $n = 3.3$ for the leading states. These parameters can be compared with the experimental values given above. The p_T^2 distribution shown in fig. 3 is well represented by the Lund calculation.

From this study we therefore conclude:

(a) The inclusive cross section for D meson production with $x_F > 0$ is $(15.8 \pm 2.7)\mu b$. This is somewhat higher than the first order predictions of the fusion calculations.

(b) A leading component to the x_F distribution is observed representing ~ 20% of the cross section. This effect is not predicted by the simple fusion calculations however a fusion calculation using the Lund fragmentation gives a reasonable fit to the data.

The central or non-leading part of the x_F distribution is well reproduced by all three fusion calculations considered.

(c) The transverse momentum distribution is well reproduced by either the Lund calculation or the bare QCD fusion calculation.

A leading particle effect in D-meson production in $\pi^- p$ at SPS/FNAL energies has been reported in previous experiments [2,15] and in the light of the data given here must be considered as established.

Acknowledgements

We would like to acknowledge the hardware specialists of the bubble chamber crew and the SPS and the painstaking work of the scanning staff at the collaborating laboratories for their contribution to the data selection. In addition, we thank H. Baer, V. Barger, R. Phillips, H.U. Bengtsson and G. Gustafson for illuminating discussions of the theoretical models.

Finally we would like to thank the various funding agencies of our collaboration for making this work possible.

REFERENCES

[1] M. Aguilar-Benitez et al. (to be published in Z. Phys. C (1985)).

[2] M. Aguilar-Benitez et al., Phys. Lett. 123B (1983) 98.

[3] W.W.M. Allison et al., Nucl. Instr. & Meth. 224 (1984) 396.

[4] M. Aguilar-Benitez et al., Phys. Lett. 135B (1984) 237.

[5] R. Klanner, XXII International Conference on High Energy Physics Leipzig 1984, p. 201.

[6] M. Aguilar-Benitez et al., D^* production in 360 GeV/c π^-p interactions (to be published in Phys. Lett. (1985)).

[7] H. Baer and A. Gurtu, NA27 Internal Note.

[8] D.W. Duke and J.F. Owens, Phys. Rev. D30 (1984) 49;
J.F. Owens, Phys. Rev. D30 (1984) 943;
J.F. Owens and E. Reya, Phys. Rev. D17 (1978) 3003.

[9] G. Altarelli, Phys. Lett. 76B (1978) 89.

[10] B. Cox and P.K. Malhotra, Phys. Rev. D29 (1984) 63.

[11] C. Peterson, D. Schlatter, I. Schmitt and P. Zerwas, Phys. Rev. D27 (1983) 105.

[12] B. Andersson, H.U. Bengtsson and G. Gustavsson, LUND TP 83-4 (1983);
H.U. Bengtsson and G. Ingleman, LUND TP 84-3/CERN/TH 3820 (1984).

[13] C.E. Carlson and R. Suaya, Phys. Rev 18 (1978) 760 and Phys. Lett. 81B (1979) 329.

[14] S.N. Ganguli and M. Schouten, Z. Phys. C. Particles and Fields 19 (1983) 83.

[15] J.L. Ritchie et al., Phys. Lett. 138B (1984) 213.

FIGURE CAPTIONS

Fig. 1 The differential distribution x_F for all D mesons having $x_F > 0$. Curve (a) is the two component fit to the data as described in the text. Curve (b) is the prediction of the Lund fusion calculation. Curve (c) is the prediction of the bare QCD fusion calculation (δ-function fragmentation). Note that both theoretical curves have been normalised to the observed total cross section for $x_F > 0$.

Fig. 2 (a) The differential distribution in x_F for "non-leading" quark states. The solid curve (a) corresponds to the single component experimental fit with $n = 7.9^{+1.6}_{-1.4}$ as given in the text. The dotted curve (b) is the prediction of the Lund calculation.

(b) The differential distribution in x_F for the "leading" quark states. The solid curve (a) is a two component fit to the data with the central component exponent n_1 fixed from the fit to the "non-leading" states. The leading component has $n_2 = 1.0^{+0.9}_{-0.7}$. The dotted curve (b) is the prediction of the Lund calculation for the leading states. Note that the Lund calculation is normalized to the total cross section for $x_F > 0$, i.e. the sum of the leading plus non-leading cross sections.

Fig. 3 The differential distribution in p_T^2. The solid curve is the experimental fit of the form $d\sigma/dp_T^2 \propto \exp[-\alpha p_T^2]$ with $\alpha = 1.18^{+0.18}_{-0.16}$ $(GeV/c)^{-2}$. Curve (a) is the prediction of the Lund calculation and curve (b) is the prediction of the bare QCD calculation. The theoretical curves are again normalised to the observed total cross section for $x_F > 0$.

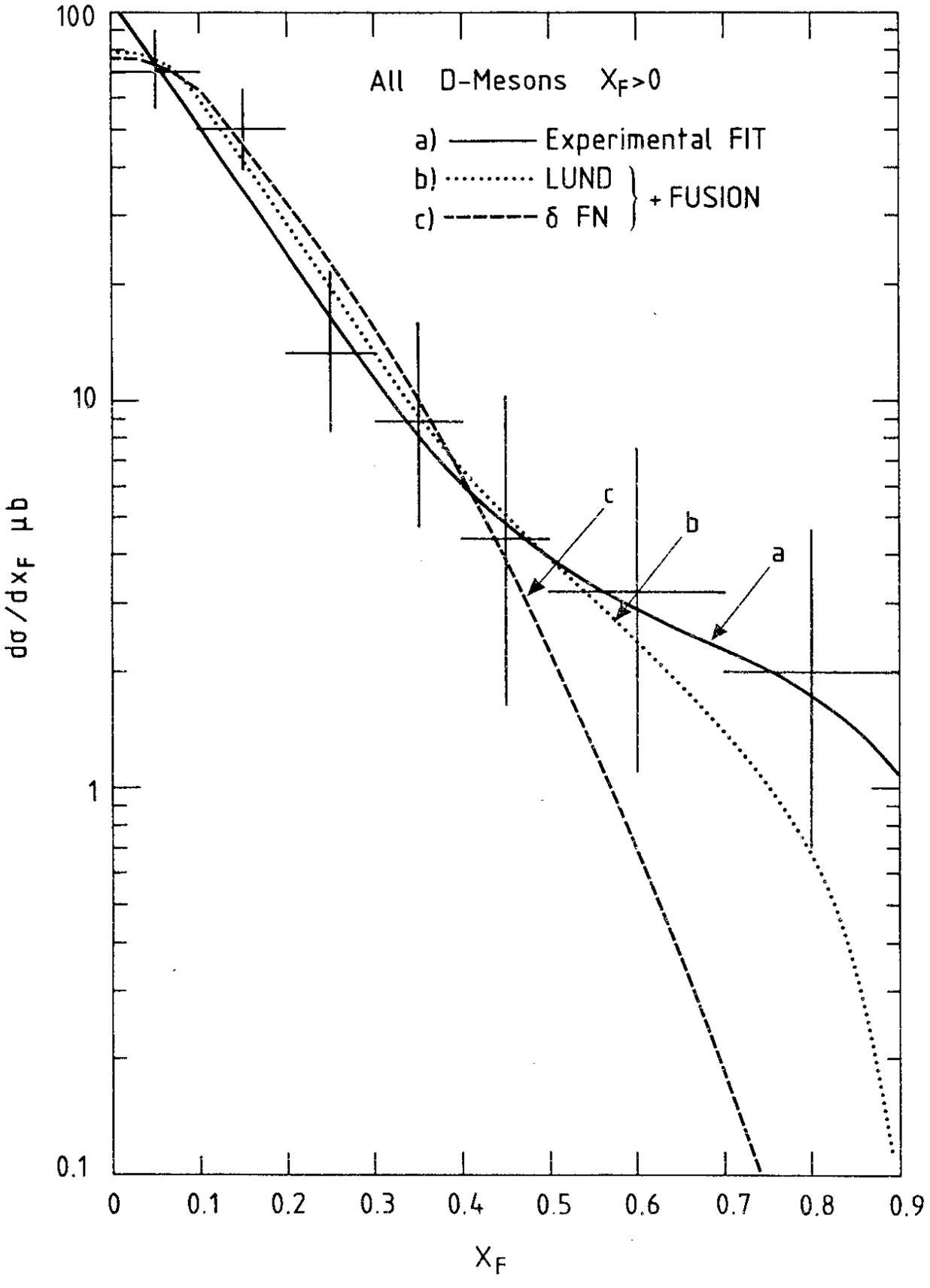
All D-Mesons $X_F>0$
a) Experimental FIT
b) LUND
c) δ FN
+ FUSION
a
b
c
100
10
1
0.1
0
0.1
0.2
0.3
0.4
0.5
0.6
0.7
0.8
0.9
$d\sigma/dx_F$ μb
X_F

Fig. 1

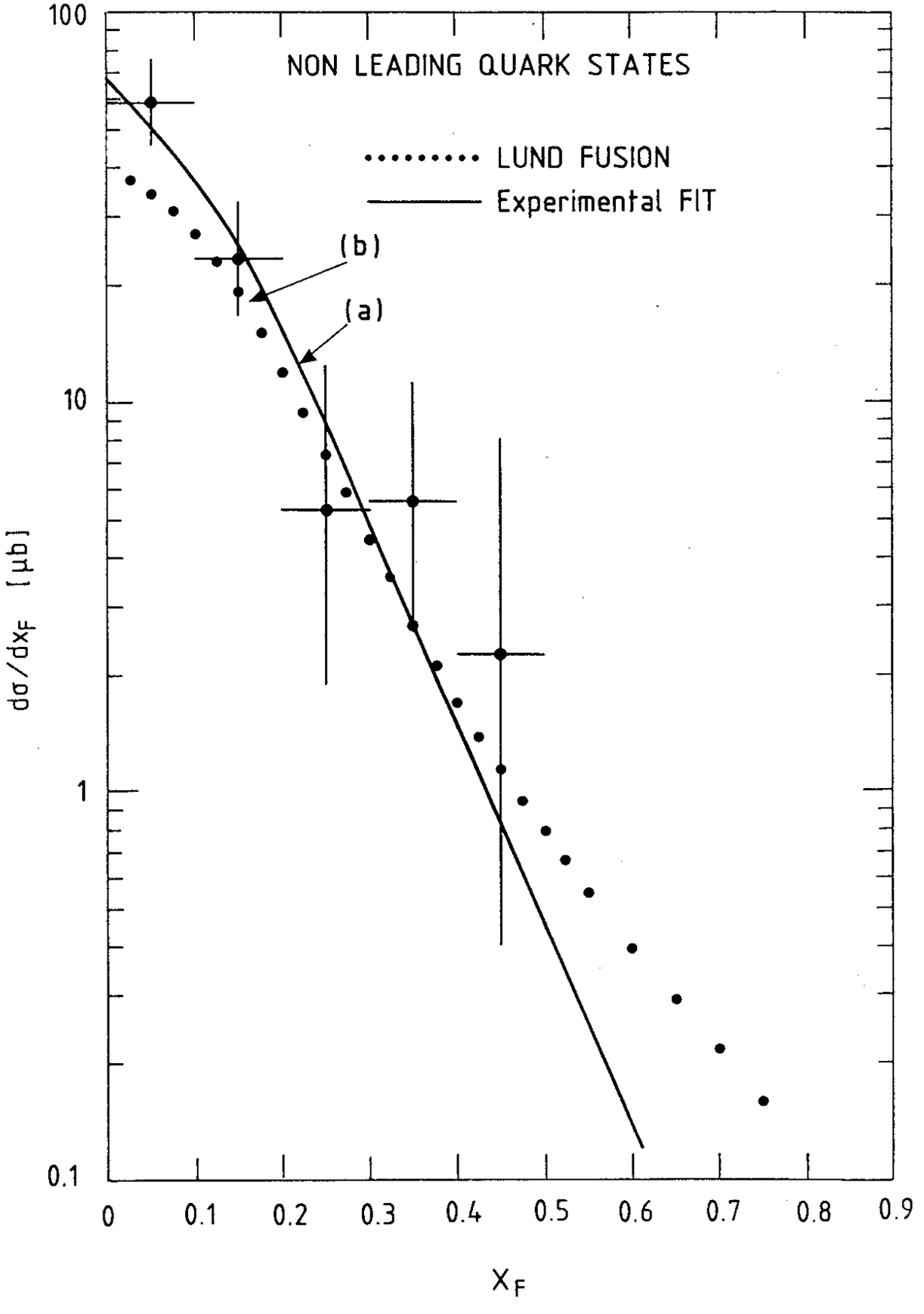
NON LEADING QUARK STATES
LUND FUSION
Experimental FIT
(b)
(a)
100
10
1
0.1
dσ/dx_F [μb]
0
0.1
0.2
0.3
0.4
0.5
0.6
0.7
0.8
0.9
X_F

Fig. 2(a)

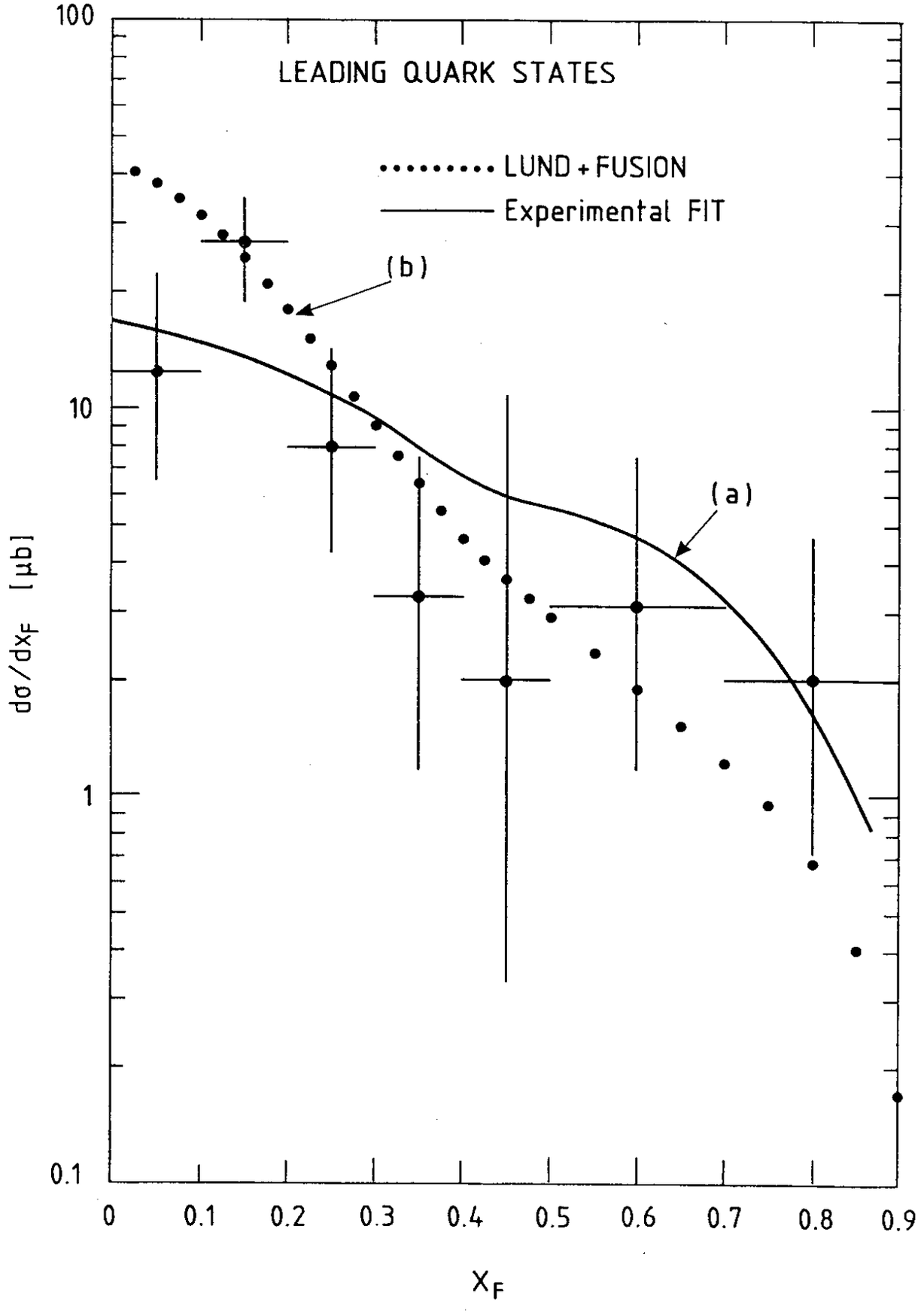
LEADING QUARK STATES
LUND + FUSION
Experimental FIT
(b)
(a)
100
10
1
0.1
0
0.1
0.2
0.3
0.4
0.5
0.6
0.7
0.8
0.9
dσ/dx_F [μb]
X_F

Fig. 2(b)

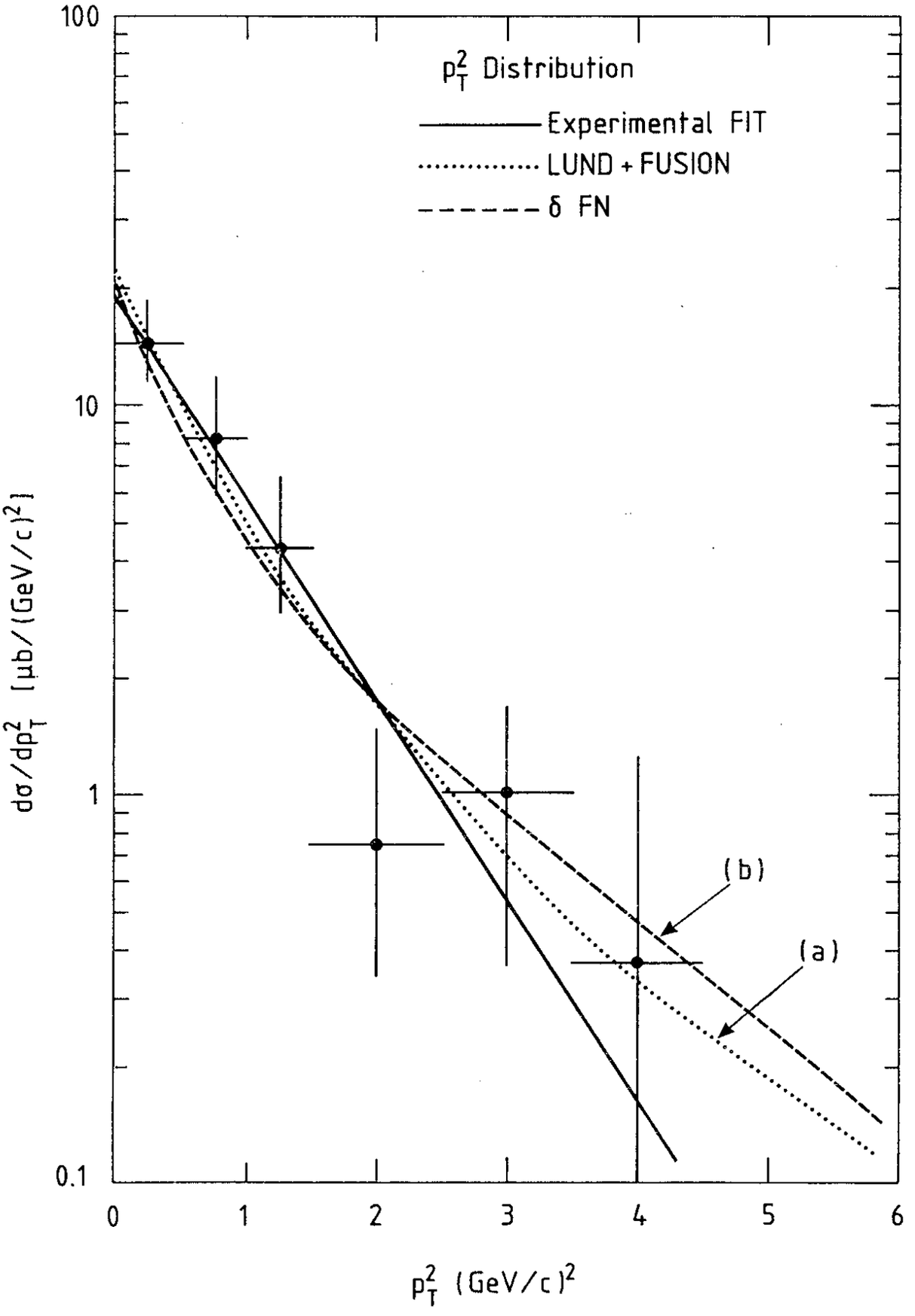
p_T^2 Distribution
Experimental FIT
LUND + FUSION
δ FN
(b)
(a)
100
10
1
0.1
0
1
2
3
4
5
6
$d\sigma/dp_T^2$ [μb/(GeV/c)^2]
p_T^2 (GeV/c)^2

Fig. 3